

Non-Small Cell Lung Tumor Identification by CNN and ANN Classifier

P.Jagadeesh¹, V.S Jayanthi², Radhika Bhasker³

¹Assistant Professor, Department of ECE, Saveetha School of Engineering, SIMATS, Chennai-602105, Tamilnadu

²Professor, Department of ECE, Rajagiri School of Engineering & Technology, Kakkanad, Kochi 682

³Associate Professor, Department of ECE, Saveetha School of Engineering, SIMATS, Chennai-602105, Tamilnadu

ABSTRACT

Non-Small Cell Lung Cancer (NSCLC) is a significant cellular degeneration of the lungs. The appropriate conclusion depends on the planning and evaluation of the tumor. Neurotic expectations often lead to complications due to the discovery of inhibition of tissue testing. AI techniques can play an essential role in such situations. Deep Neural Networks (DNNs) have become new entities in this space. The leading cause of pulmonary cell failure is non-small cellular collapse (NSCLC). Many of the most important efforts to date have been made for the mechanical use of NSCLC, but the successful use of neural networks will still be evident in this study area. DNN is poised to perform more critical accuracy than conventional neural organizations as it uses other convolutional layers organization (CNN). The current investigation proposes a CNN-based and fast-paced model of joining an intermittent neural organization (ANN) programming with the NSCLC robot and comparing the result with a few AI statistics and some comparative research. NSCLC is a multidisciplinary radiogenomics from a growing database (TCIA). Image inputs were refined and filtered by resizing, enlarging, removing sound, etc. The image below the preparation section was followed by a presentation based on the image above. Separated images are maintained by including location and output models involved in two consecutive phases: extremely stable locations and mass exposure after delayed analysis; CNN-ANN is ready for the model to be determined and selected designated points for the model. The proposed CNN-ANN model almost hit some useful AI statistics. Accuracy remained consistently high than other modern tests. The proposed CNN-ANN model performed very well during the investigation. Additional tests may be completed by model reorganization and forming a selected emotional support network of oncologists and radiologists. Further research can be done by considering limited study or study methods alone.

Keywords—Deep Learning Algorithm, Lung Cancer, NSCLC, MR Images.

Article Received: 10 August 2020, Revised: 25 October 2020, Accepted: 18 November 2020

Introduction

Pulmonary cell death is perhaps the most deadly and frightening disease in the world. Multiple pulmonary cell degeneration is a form of non-small cell injury (NSCLC) [1]. Different types of NSCLC [2] are adenocarcinoma, squamous cell carcinoma, large cell carcinoma, etc. Close discovery, systematic planning, and screening [3] tumors or injuries are also very different from defining an appropriate adverse treatment program [4]. One of the most common ways to improve direct damage is the tumor-node-metastasis (TNM) planning framework [5]. The content is distinguished by italic sort, inside sections, following the model. For example, different things, such as staggered details, graphs, and tables, are not set, albeit various table content styles are given. The configuration should make these segments, including the appropriate

accompanying conditions. The American Joint Cancer Committee (AJCC) planning can be considered to consider better TNM planning [6]. Such arrangements can have a profound effect on identifying a collection or collection. Several circles have successfully investigated a new plant-based system to improve the concentration and transmission of incomplete radiation through flexible tissues [7] [9]. Lung tissue has a unique follow-up premium due to its high mobility capacity during treatment delivery. Studies have shown that lung tissue can rise in the sub-par prominent, the front and back, and the left when normal breathing is performed [10] [11]. In [8], visual cues showed the detection of intrafraction lung-tumor following the use of Siemens leaf multi-leaf collimator (MLC) and Varian leaf MLC, respectively. The tumor agent was performed in both studies following a sinusoidal guideline, and

its position was approved by a movement testing framework developed by Calypso Medical Technologies. Cho et al. proposed the simultaneous use of subsequent kV / MV imaging, in which the gold mark was used as a contract. Towards the end of time, Cervino et al. point out that there may be a focus on MRI-directed lung tissue following traces of cine-MR volunteer arteries that exploit linac-MR MR imaging statistics presented in our laboratory [12 - 15]. Unless the system tracking is subject to change, using an online MLC control strategy (e.g., not pre-programmed movement) for standard monitoring is permitted. Ideally, the following can provide standard targeted identification and bar delivery. However, there is an unavoidable structural delay between the two periods due to (1) the time required to drive each MLC leaf in the allotted area and (2) the registration/preparation time. The newly announced frame adjusts the range from 160 to 500 ms until the next day. Due to the long heartbeat with a movement speed known as 4-94 mm / s, an independent delay of 500 ms can result in a plant boundary disturbance of up to a maximum of 47 mm. Given this inevitable structural delay, anticipating crop movement strategy is an excellent idea to minimize closure errors. Various statistics have been suggested to predict plant movement during adjustment delays [16 - 16]. Because of the unusual type of lung and tumor movement that reflects the speed and frequency of changes, some circles have explored the use of nonprofit organizations (ANNs) for predicting movement [19] [20]. Although this investigation is promising, based on subsequent MRI. First, the ANN exhibition is known for its unwavering reliance on its design and delivery loads (IW) [21] [22] [23]. Verma et al., That is, ANN engineering must be developed to be used to anticipate plant movement. However, there are no previous studies on the expected lung movement to investigate this problem. Second, previous studies accepted the tumor location at 30 Hz by looking at the external or internal tumor replacement position using the following optical devices or the stereoscopic x-

beam fluoroscopy system. Pulmonary movements, intrathoracic tissue, connections, etc., can achieve a shot to protect the casings' image per second (fps). This level is elevated by continuous follow-up of lung-tumor movement and can be done using our current linac-MR. No previous studies have been performed and tested to anticipate lung-tumor move using an MRI-supported tumor.

To conquer these issues, we propose a lung-tumor development file dependent on CNN-ANN for MRI-based intrafractional lung-tumor following. This report plots the CNN-ANN program, vital arranging, more CNN-ANN advancement, and improved CNN-ANN design and IW programs. Our record's normal explicitness was surveyed utilizing information from 29 cell degeneration in lung patients with shifting draft cracks.

RELATED WORK

Clinical biomarkers offer the benefits of being a non-invasive method and produce an utterly abnormal tumor instead of blocked tissue accessible by biopsy [24]. After that, setting up the AJCC with a robot could play a significant role in navigating as a full-time network assistant to a health care professional. Such robotization will also not have a TNM structure. AI processes can help in the use of such a scale of robots. Among the most complex AI processes, the Artificial Neural Network (ANN) can be a systematic decision as it empowers the machine to accept the human thought process. A typical neural implant model (ANN) may suffer from problems such as extensive data processing, increased PC scale, longer study routes [25], and more accurate State-of-work-workmanship can be done with a deep neural organization (I - DNN) as it uses additional layers of the convolutional neural organization (CNN) [26]. The construction of a standard DNN site can include the following: INPUT layer containing the highlights from the target image, the CONVOLUTION layer registers the yield of particles corresponding to the surrounding areas in the information, the fixed layer (RELU) uses the intellectual object -FC (for

example fully connected) layer lists school scores. Many vital programs have already begun with computer space or deteriorating lung cell deficiency with CNN [27 - 29]. In 2017, Teramoto et al. performed the mechanical segregation of NSCLC using DNN and was stabilized with approximately 71% accuracy. That same year, Rossetto and Zhou destroyed several lung cells, although their DNN model showed high clarity, not sensitive clinical data.

In 2018, Chaunzwa et al. made a twofold arrangement of NSCLC histology utilizing top to bottom investigation radionics and acquired 75% exactness. In 2018, Coudray et al. altered and arranged NSCLC utilized the profundity of learning with high precision; however, it just tests the sub-organization of the NSCLC. In the same year, Serj et al. 87% exactness was accomplished in a similar report zone. In 2019, Yu et al., regardless of whether the characterization of NSCLC histopathology species utilizes DNN. None of the previously mentioned issues center on fixing or restoring tissue or injury of NSCLC. They try to complete the prediction using location data directly from 2-D or 3-D images, creating a standard image separation problem. The immediate promise that these tests were achieved was to determine whether the bio-clinical picture (2-D or 3-D) was NSCLC or not. Therefore, this study used 2-D or 3-D Convolution layers that revealed machine design and time value. Therefore, there is a need for extensive research to provide information on simple but effective DNN models that can play a role in the NSCLC AJCC planning.

Consequently, it may help make clinics fully aware of NSCLC, and they may have the option to deviate from the treatment process with the worst possible accuracy. The big problem with the construction of CNN is that it has no memory; then again, the recurrent neural organization (RNN) has an input ring that is well equipped to recall past events. This could help improve the proposed model's overall accuracy if CNN could be used as a pre-ANN preparation business [31-34]. The new model will then be CNN-enabled

memory. The conversion process is set by the tradeoff between Convents speed and fun and the impact of ANN request. Figure 1 portrays System Model of the Proposed CNN-ANN Model

SYSTEM METHODOLOGY

The experiment's real purpose was to make the AJCC (seventh edition) connection of the NSCLC using the necrossoveral corporate organization (CNN) crossover and RNN. The in-depth learning strategy has hit the standard formation of neural organization and many other AI driving modes in many events. Large numbers of current trials were suggested for a simple diagnosis of lung cancer as positive or threatening using a convolutional neural association or general neural association. The recent study is characterized by describing a straightforward yet practical model of the Deep Learning Model integrated with the ANN developed by NSCLC with a high degree of clarity. The focus also analyzes the effect of the proposed model with a few key AI statistics alongside a few previous comparative tests. The picture preparation for the investigation submission was completed using MATLAB, and various data mining activities were carried out using WEKA. The CNN-ANN model was created and implemented in Python with a tensor flow at the end of the camera API library. The other paper is divided into related categories: strategies, data protection, image editing, extraction, analysis, effect, expiration, and future expansion. Such tests are sometimes reflected in the better details of the analysts of the current investigation. In stark contrast to the modern research-based on NSCLC head-to-head mechanization, the present experiment has embraced all involved.

To perform automated isolation of NSCLC pictures first and afterward accomplish the plan of bubbles or sores of the influenced images. The current examination isolated the territory information from a different bump, fused it into the clinical for information altering, and utilized the CNN-ANN hybrid model to accumulate the knowledge. For example, the test used area information, Tensor data implanted in a comma solo record (CSV). The two tensors' position

includes details (line, segment), although the role of the three tensors has details, for example (line, part, shading channels). Like this, the initial component of the model is comprised of Convolutional layers, trailed by layers of the mix. The show can offer a speedy and humble alternative, not at all like a dull association. Likewise, Conv1D layers are utilized as pre-preparing layers when their yields were kept up at ANN. The proposed CNN-ANN model comprises a solitary one-Dimensional addition layer followed

by shrouded layers of one-dimensional close to a solitary article and a solitary thick layer. The provocative layer changes over the Three-Dimensional yield into a Two-Dimensional result. One-Dimensional layer MaxPooling runs through each Convolutional layer. The 1-Dimensional integration layer supports One-Dimensional-related data. The CNN crop was maintained by a duplicate unit layer (GRU, [25]) rather than a temporary memory layer

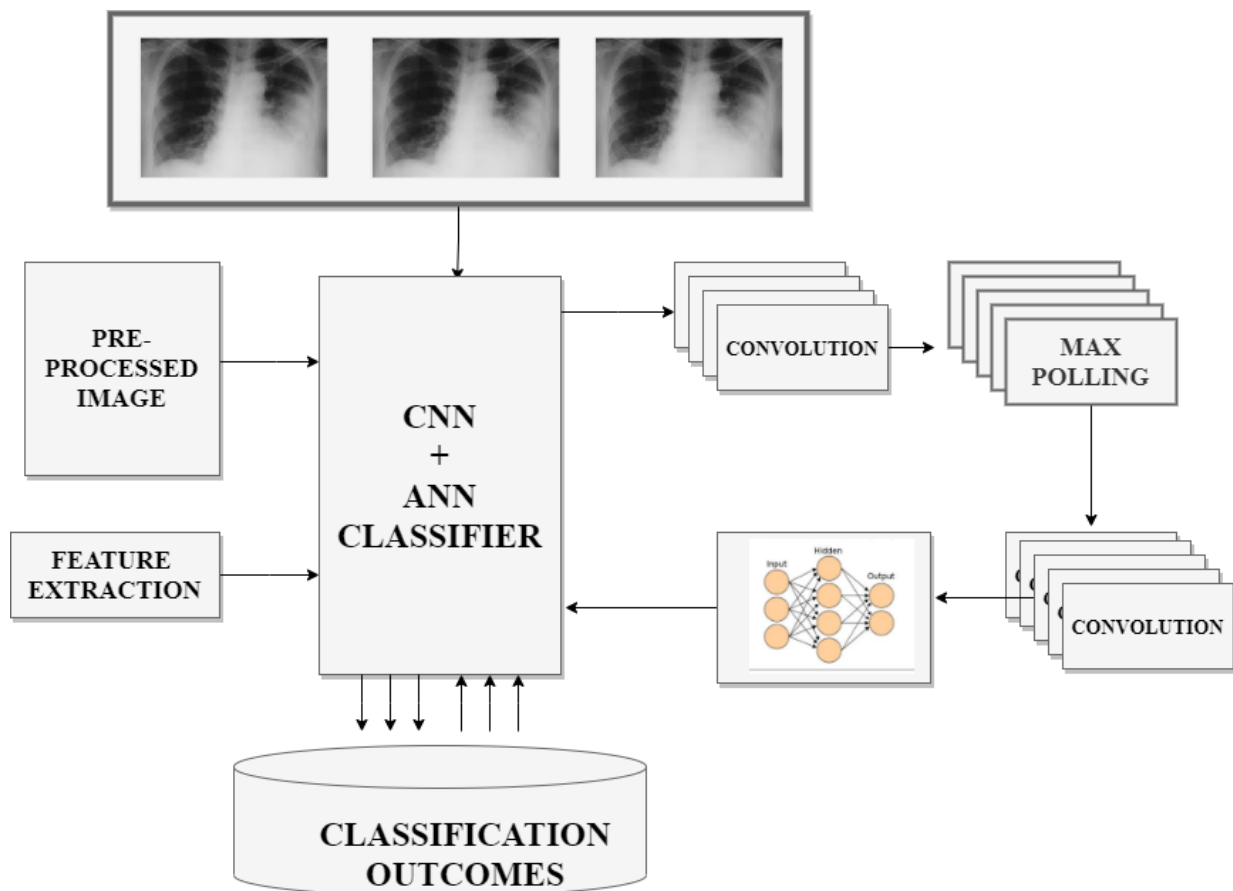


Figure 1: System Model of the Proposed CNN-ANN Model

TABLE 1: EVALUATION METRICS OF DIFFERENT ALGORITHMS

TECHNIQUE	F-MEASURE	PRECISION	RECALL	ROC AREA
DNN	0.756	0.748	0.773	0.876
RNN	0.821	0.814	0.823	0.876
ANN	0.89	0.88	0.892	0.945
CNN	0.94	0.93	0.93	0.956
CNN+ANN	0.97	0.97	0.965	0.987

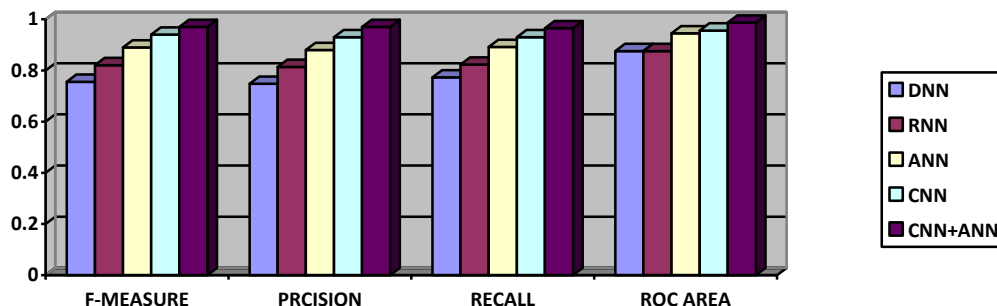


Figure 2: Evaluation Metrics of the Proposed CNN-ANN Model with other Algorithms

TABLE 2: ACCURACY RATE OF THE PROPOSED CNN-ANN MODEL WITH OTHER ALGORITHMS

S.NO	TECHNIQUE	ACCURACY RATE (%)
1	DNN	0.786
2	RNN	0.841
3	ANN	0.898
4	CNN	0.94
5	CNN+ANN	0.98

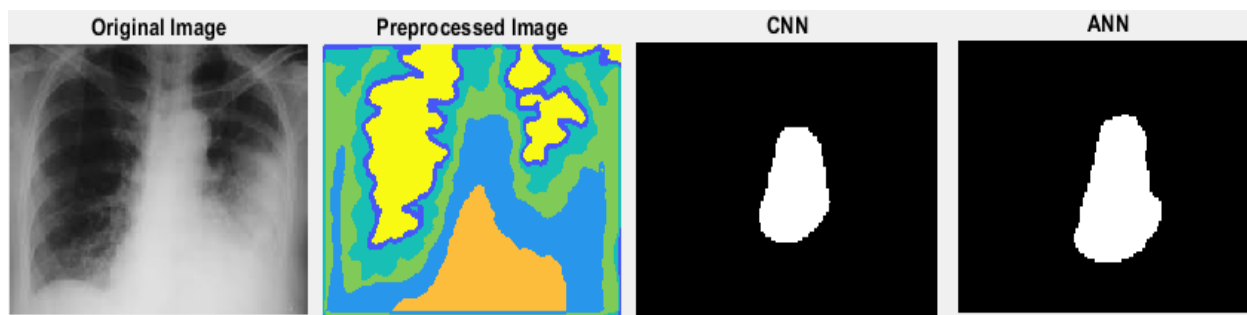


Figure 3: Classification Outcomes for the Proposed CNN-ANN Model

(LSTM, [26]). This is done as the GRU layer is heavier than LSTM and carries LSTM features. The following is a thick layer that is closely related. A completely related layer thinks of all the unthinkable. The thick coating is currently 2-D naturally; (Extract in parent layer, channel size); all Conv1d or GRU layers have 3-D shapes, for example (Extract in parent layer, channel size, Channel number). Since the thick layers and their archetypes are incompatible, the inflammatory layer is introduced in the middle. The yield from the GRU layer is maintained in the dense layer. Finally, there is a thick yield layer with the sigmoid starting function of using phase scores.

EXPERIMENTAL RESULTS AND DISCUSSION

Effective clinical thinking processes can be straightforward due to the nature of the mechanical damage. They can differentiate or a limited number of changes in the chemical structure in chemical structure. Increasingly, the production of imaging techniques, for example, Positron Emission Tomography (PET), will not help with the misuse of chemicals. In this way, visual biological evidence can be strengthened if imaging techniques are incorporated into the club with basic imaging techniques, for example, processed tomography (CT). Multimodal imaging methods, for example, PET / CT, may have the

option of seeing a specific region of benefit for any event, with a small tumor or a measured lesion. The NSCLC Radio genomics Collection from The Cancer Imaging Archive (TCIA) is considered for testing. The variety contains photos of the PET/CT (DICOM) tumor of 211 patients. Treatment data (CSV) was obtained to acquire significant AJCC arranging data concerning every tumor or lesion influenced. The assortment has 1355 edits and 285,411 photographs. This database is designed to promote event-based retrieval and biomarker testing of a predictive clinical picture. Treatment details include side effects of treatment, genomics, pathology, and so on. Table 1 portrays the evaluation metrics of different algorithms. Figure 2 predicts the Evaluation Metrics of the Proposed CNN-ANN Model with other Algorithms

A. Feature Extraction and Pre-Processing

Image classification is bypassed by a few pre-rendered image processing tasks such as enhancement or sharpening, blurring, stopping the noise, edge area, etc. At the time of segregation, high sensitivity was controlled using Otsu's histogram strategy. The method based on the foundation was obtained with the help of the behavioral markers of the affected plant images. The shape and the boundary based on the face were used to distinguish the same pixel fusion, and the Circuit of Interest (RoI) was given accordingly. The degree of separation is determined by the stage of release of the object. Extremely stable external zones (MSER) were used to identify the dominant elements, and subsequently, the most vital points (SURF) were used to subtract underserved points.

B. Discussions

Highlights from the previous section are sent to the club with clinical information available from TCIA. Excess details, for example, patient component details, etc. It was physically discarded. Therefore, only the neurotic data identified by the AJCC (version seven) of all patients were taken from clinical information and combined with different themes to form a final database. The flexibility of the AJCC structure is

considered a phase or target variable. All non-numerical and complex numeric features in the database have been replaced by methods (relevant information) and procedures (numerical information) from the configuration information. Initially, the database was independently set to $[-1, 1]$ and then rated at $[0, 1]$. CNN (Modification of model without repetition layer) and distinct statistics (Table 3a). Bench specification showed an undeniable quality of the CNN-RNN model when set through a fixed database. Position analysis reveals the unparalleled quality of the CNN-RNN model over CNN and many techniques. The experiment was completed with a set of data while leading to a last-minute deadline; the database was modified several times to separate the priorities' impact. The accuracy of the AJCC layout was estimated to be CNN-ANN (standard database), and the result was comparable to a few essential AI methods, for example, the closest neighbor to K (KNN), rare backwoods (RF), see vector machine (SVM) and multilayer layer perceptron (MLP). The 10-Fold cross-approval strategy has been applied to the database, and the accuracy of the model and bad luck has always been well documented. All tests were performed using Intel (R) Core (TM) CPU centers for 32-3230 m Computer chip @ 2.60 GHz processor using standard data set. After ten redesigns, the information didn't show a lot of progress in the split outcomes. For each altered data set, every one of the five AI steps is performed with 10-Fold authorization data. Accuracy has recorded all the figures in each emphasis. Finally, the precise definition of each plan was determined alongside the general variance. Figure 3 displays Classification Outcomes for the Proposed CNN-ANN Model and Figure 4 predicts the Accuracy Rate of the Proposed CNN-ANN Mode

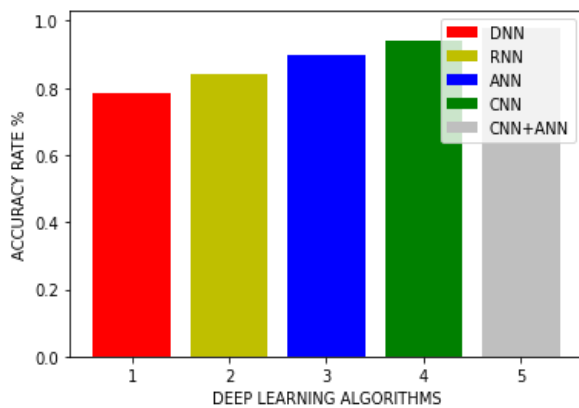


Figure 4: Accuracy Rate of the Proposed CNN-ANN Model

CONCLUSION

After considering the final test result, it can be assumed that the proposed CNN-ANN model performed more efficiently compared to other active AI strategies. CNN-ANN's average rating was 98.2% higher than its closest rival to timberland 89%. Likewise, the exactness during the testing stage was consistently equivalent to precision during the readiness stage. Lamentably, during the planning stage the distance was not an issue during the test stage. It was also found that the proposed CNN-ANN model was consistently superior to other applicable AI statistics. Accuracy was consistent during measurement and repetition height. The standard deviation of CNN-ANN was additionally on the lower side than the different figures. The proposed CNN-ANN model's high exactness has shown its capacity to perform more precisely in disposing of a multiclass issue than other standard AI computations. Typical deviations were lower due to having a more accurate level of accuracy than various calculations. SVM and different general AI strategies are best suited for two order issues. Investigations point to their shortcomings due to a multi-level problem like the current one. Since the test's recent prominence had real numerical properties with few comparisons, these techniques couldn't function admirably. These thoughts mirrored the elements of the proposed model. It doesn't make any difference whether we consider other significant assessment estimates. For example, Cohen's Kappa Statistics or Receiver

Operating Curve (ROC), and so on, we can discover the proposed CNN-ANN model's consistency and productivity. Let us investigate part of the comparative investigation and their evaluation of the current research. From the release, it is clear that the CNN-ANN model used in the recent study has the edge of other driving tests targeted at the comparison site. Such an organization may be further prepared to achieve a better outcome in the planning and learning of the NSCLC. Such tests can help prepare for NSCLC treatment, and help analysts remove better-computerized oncology testing in the future.

Future Directions And Issues

While looking for a simple but effective DNN, research has suggested a slightly targeted CNN-ANN model. Additional testing may lead to the completion of various strategies, for example, from a long-term network (LSTM) Network or a Bi-directional repetitive neural organization, etc. The current study was classified as NSCLC. Comparative tests may be performed in the future with various fatal strains, for example, asthma or other diseases, etc. The examination focused on CT images only. Later on, different kinds of multimodal biomedical imaging, for instance, MRI-PET, and so forth. They can likewise be set under the space of such tests.

References

- [1] Alberg AJ, Brock MV, Stuart JM. Epidemiology of lung cancer: looking to the future. *J Clin Oncol*. 2005;23:3175–85.
- [2] Horn L, Eisenberg R, Gius DR, Kimmelschue KN, Massion PP, Putnam JB, Robinson CG, Carbone DP. Cancer of the lung: non-small cell lung cancer and small cell lung cancer. In: *Abelof's Clinical Oncology: the fifth edition*. Elsevier Inc; 2013. pp., 1143–1192. <https://doi.org/10.1016/B978-1-4557-2865-7.00072-2>.
- [3] Gleason DF, Mellinger GT. Prediction of prognosis for prostatic adenocarcinoma by combined histological grading and clinical

- staging. *J Urol.* 2002;167(2 Pt 2):953–8. [https://doi.org/10.1016/s0022-5347\(02\)80309-3](https://doi.org/10.1016/s0022-5347(02)80309-3) discussion 959.
- [4] Nivetha P, Manickavasagam R. Lung cancer detection at an early stage using PET/CT imaging technique. *Int J Innov Res Comput Commun Eng.* 2014;2(3):358–3363.
- [5] Brierley JD, Gospodarowicz MK, Wittekind Ch, editors. *TNM classification of malignant tumours.* 8th ed. Chichester: Wiley-Blackwell; 2017. ISBN 978-1-4443-3241-4.
- [6] Zahoor H, Luketich JD, Weksler B, Winger DG, Christie NA, Levy RM, Gibson MK, Davison JM, Nason KS. The revised American Joint Committee on Cancer staging system improves prognostic stratification after minimally invasive esophagectomy for esophagogastric adenocarcinoma. *Am J Surg.* 2015;210(4):610–7. <https://doi.org/10.1016/j.amjsurg.2015.05.010>.
- [7] M. B. Tacke, S. Nill, A. Krauss, and U. Oelfke, "Real-time tumour tracking: Automatic compensation of target motion using the Siemens 160 MLC," *Med. Phys.* 37(2), 753–761 (2010).
- [8] A. Sawant, R. L. Smith, R. B. Venkat, L. Santanam, B. C. Cho, P. Poulsen, H. Cattell, L. J. Newell, P. Parikh, and P. J. Keall, "Toward submillimeter accuracy in the management of intrafraction motion: The integration of real-time internal position monitoring and multileaf collimator target tracking," *Int. J. Radiat. Oncol., Biol., Phys.* 74(2), 575–582 (2009).
- [9] B. Cho, P. R. Poulsen, A. Sloutsky, A. Sawant, and P. J. Keall, "First demonstration of combined Kv/Mv image-guided real-time dynamic multi-leaf collimator target tracking," *Int. J. Radiat. Oncol., Biol., Phys.* 74(3), 859–867 (2009).
- [10] H. Shirato, Y. Seppenwoolde, K. Kitamura, R. Onimura, and S. Shimizu, "Intrafraction tumour motion: Lung and liver," *Semin. Radiat. Oncol.* 14(1), 10–18 (2004).
- [11] C. Plathow, C. Fink, S. Ley, M. Puderbach, M. Eichinger, I. Zuna, A. Schmahl, and H. U. Kauczor, "Measurement of tumour diameter dependent mobility of lung tumours by dynamic MRI," *Radiother. Oncol.* 73(3), 349–354 (2004).
- [12] A. Krauss, S. Nill, M. Tacke, and U. Oelfke, "Electromagnetic real-time tumour position monitoring and dynamic multileaf collimator tracking using a Siemens 160 MLC: Geometric and dosimetric accuracy of an integrated system," *Int. J. Radiat. Oncol., Biol., Phys.* 79(2), 579–587 (2010).
- [13] B. G. Fallone, B. Murray, S. Rathee, T. Stanescu, S. Steciw, S. Vidakovic, E. Blosser, and D. Tymofichuk, "First MR images obtained during megavoltage photon irradiation from a prototype integrated linac-MR system," *Med. Phys.* 36(6), 2084–2088 (2009).
- [14] J. Yun, E. Yip, K. Wachowicz, S. Rathee, M. Mackenzie, D. Robinson, and B. G. Fallone, "Evaluation of a lung tumour auto contouring algorithm for intrafractional tumour tracking using low-field MRI: A phantom study," *Med. Phys.* 39(3), 1481–1494 (2012).
- [15] J. Yun, M. MacKenzie, D. Robinson, S. Rathee, B. Murray, and B. G. Fallone, "Real-time MR tumour tracking using a Linac-MR system," in *Proceedings of the 56th Annual Meeting of the COMP, Ottawa, ON, June 16–19, 2010.*
- [16] G. C. Sharp, S. B. Jiang, S. Shimizu, and H. Shirato, "Prediction of respiratory tumour motion for real-time image-guided radiotherapy," *Phys. Med. Biol.* 49(3), 425–440 (2004).
- [17] A. Krauss, S. Nill, and U. Oelfke, "The comparative performance of four respiratory motion predictors for real-time tumour tracking," *Phys. Med. Biol.* 56(16), 5303–5317 (2011).

- [18] P. S. Verma, H. M. Wu, M. P. Langer, I. J. Das, and G. Sandison, "Survey: Real-time tumour motion prediction for image-guided radiation treatment," *Comput. Sci. Eng.* 13(5), 24–35 (2011).
- [19] J. H. Goodband, O. C. L. Haas, and J. A. Mills, "A comparison of neural network approach for online prediction in IGRT," *Med. Phys.* 35(3), 1113–1122 (2008).
- [20] M. J. Murphy and D. Pokhrel, "Optimization of an adaptive neural network to predict breathing," *Med. Phys.* 36(1), 40–47 (2009).
- [21] H. R. Maier and G. C. Dandy, "The effect of internal parameters and geometry on the performance of back-propagation neural networks: An empirical study," *Environ. Modell. Software* 13(2), 193–209 (1998).
- [22] L. F. A. Wessels and E. Barnard, "Avoiding false local minima by proper initialization of connections," *IEEE Trans. Neural Networks* 3(6), 899–905 (1992).
- [23] C. Plathow, S. Ley, C. Fink, M. Puderbach, W. Hosch, A. Schmahl, J. Debus, and H. U. Kauczor, "Analysis of intrathoracic tumour mobility during whole breathing cycle by dynamic MRI," *Int. J. Radiat. Oncol., Biol., Phys.* 59(4), 952–959 (2004).
- [24] Napel S, Plevritis SK. NSCLC radiogenomics: initial Stanford study of 26 cases. *Cancer Imaging Arch.* 2014. <https://doi.org/10.7937/K9/TCIA.2014.X7ONY6B1>.
- [25] Breiman, Leo. Random forests. *Mach Learn.* 2001;45(1):5–32.
- [26] Szegedy C, Liu W, Jia Y, Sermanet P, Reed S, Anguelov D, Erhan D, Vanhoucke V, Rabinovich A. Going deeper with convolutions. In: *Proceedings of the IEEE conference on computer vision and pattern recognition*; 2015. pp. 1–9.
- [27] Teramoto A, Tsukamoto T, Kiriya Y, Fujita H. Automated classification of lung cancer types from cytological images using deep convolutional neural networks. *BioMed Res Int.* 2017;20:17. <https://doi.org/10.1155/2017/4067832>.
- [28] Chaunzwa TL, Christiani DC, Lanuti M, Shafer A, Diao N, Mak RH, Aerts H. Using deep-learning radionics to predict lung cancer histology. *J Clin Oncol.* 2018;36(15):8545. https://doi.org/10.1200/jco.2018.36.15_suppl.8545.
- [29] Rossetto AM, Zhou W. Deep learning for categorization of lung cancer CT images. In: *2017 IEEE/ACM international conference on connected health: applications, systems and engineering technologies (CHASE)*, Philadelphia, PA; 2017. pp. 272–273. <https://doi.org/10.1109/chase.2017.98>
- [30] Coudray N, Ocampo PS, Sakellaropoulos T, Narula N, Snuderl M, Fenyö D, Moreira AL, Razavian N, Tsirigos A. Classification and mutation prediction from non-small cell lung cancer histopathology images using deep learning. *Nat Med.* 2018;24(10):1559.
- [31] Abraham, G. K., Jayanthi, V. S., & Bhaskaran, P. (2020). Convolutional neural network for biomedical applications. In *Computational Intelligence and Its Applications in Healthcare* (pp. 145-156). Academic Press.
- [32] Abraham, G. K., Bhaskaran, P., & Jayanthi, V. S. (2019, November). Lung Nodule Classification in CT Images Using Convolutional Neural Network. In *2019 9th International Conference on Advances in Computing and Communication (ICACC)* (pp. 199-203). IEEE.
- [33] Jayanthi, V. S., Simon, B. C., & Baskar, D. (2020). Alzheimer's disease classification using deep learning. In *Computational Intelligence and Its Applications in Healthcare* (pp. 157-173). Academic Press.
- [34] Simon, B. C., Baskar, D., & Jayanthi, V. S. (2019, November). Alzheimer's Disease Classification Using Deep Convolutional Neural Network. In *2019 9th International Conference on Advances in Computing and*

Communication (ICACC) (pp. 204-208).
IEEE.